ChemComm

Pyridine-d_5 as a ^{2}H NMR Probe for Investigation of Macrostructure and Pore Shapes in a Layered Sn(IV) Phosphonate-Phosphate Material

Journal:	*ChemComm*
Manuscript ID	CC-COM-11-2019-009254.R3
Article Type:	Communication

COMMUNICATION

Pyridine-d_5 as a ^{2}H NMR Probe for Investigation of Macrostructure and Pore Shapes in a Layered Sn(IV) Phosphonate-Phosphate Material

Received 00th January 20xx,
Accepted 00th January 20xx

DOI: 10.1039/x0xx00000x

Vladimir I. Bakhmutov[a]*, Douglas W. Elliott[a], Gregory P. Wylie[a], Abraham Clearfield[a]*, Aida Contreras-Ramirez[a], and Hong-Cai Zhou.[a,b]*

Isotropic and anisotropic motions and molecular states of pyridine-d_5, adsorbed on the surface within the pores of a layered Sn(IV) phosphonate-phosphate material (1) have been characterized thermodynamically and kinetically by solid-state NMR. The data obtained provide formulation of macrostructure and shapes of pores in 1.

Mixed metal (IV) phosphonate-phosphates[1] are widely applied as multifunctional materials in many fields of chemistry and industry,[2-4] and constantly attract the attention of chemists due to their role in separations of lanthanides from actinides in spent nuclear fuel.[5-7] In this application the free hydroxyls in phosphate groups P-OH and/or phosphonic acid moieties function as ion-exchangers.[5] However, despite the importance of such materials, their macrostructure and pore shapes have not been investigated.

In general, these materials are prepared by the hydrothermal method,[5-8] which yields the amorphous layered molecular systems with BET surface area values of 314 - 381 m^2/g [5,9] and wide distributions of pore sizes: from micro pores (≤20 Å) to large pores sizes of 250 Å. It is shown that as the fraction of phosphate groups increases, the average pore size is larger. For example, the percentage of pores larger than 50 Å in systems $M(O_3PC_6H_4PO_3)_{1-(x/2)}(O_3POH)_x{\cdot}nH_2O$ increases from just 5% for x = 0.5 to over 35% for x = 1.6.[9]

Recently, microporous material $Sn(O_3PC_6H_4PO_3)_{0.85}(O_3POH)_{0.30}$ (**1**) (Figure 1), as a representative of microporous phosphonate-phosphate system, has been characterized by solid-state NMR, powder X-ray diffraction and IR spectroscopy.[10] Pore spaces in **1** were probed by the behaviour of benzene-d_6 and pyridine-d_5 guest molecules. Note that solid-state NMR, ^{2}H NMR in particular, is the unique physical method for characterizations of solids and their dynamics.[11] In fact, ^{2}H is a spin-1 nucleus. It has a small quadrupole moment, giving rise to a quadrupole coupling constant sensitive to molecular motions with correlation times in the temperature range of -150 to +100°C. These motions affect line shapes of resonances observed in powders, the analysis of which allows identifications of motions and their characterizations, for example, in the case of guest molecules.[12,13]

The reorientations of benzene adsorbed in pores of **1** have been recognized as the well-known fast in-plane C_6 rotations. However, the behaviour of pyridine-d_5 in the pores was more intriguing and required a more detailed understanding, particularly in the context of the macrostructure and pore spaces in **1**. In fact, pyridine-containing samples have shown slow changes in time: *the increasing fraction of immobile pyridine molecules was observed in the variable-temperature ^{2}H NMR spectra on cooling*. Here we reinvestigate materials **1-Py-1.6**, **1-Py-0.6**, and **1-Py-0.2** prepared as described in the Supplementary Information (SI) to show 1.6, 0.6 and 0.2 mol of pyridine-d_5 per one mol of **1**, respectively. Samples of **1-Py-1.6** and **1-Py-0.6** were stored for two months after their preparation to allow them to reach an equilibrium state. The aim of the work is to demonstrate the application of solid-state NMR techniques to the guest pyridine-d_5 as a probe for investigating the macrostructure and pore shapes in metal phosphate-phosphonate materials.

The above-mentioned slow changes (over days) in ^{2}H NMR spectra of pyridine-containing materials, can be explained by two factors: a slow pyridine redistribution in the pores of **1**, or the pyridine, as a more aggressive (capable of H-bonding) guest than either benzene-d_6 or toluene-d_8,[10-12] causes slow structural reorganizations in **1**. This latter explanation is evident in the metal-organic frame work MIL-53(Cr), which undergoes a contraction upon benzene adsorption.[13] However, since these slow changes in **1** were not accompanied by visible spectroscopic changes ($^{31}P\{^1H\}$ MAS NMR, IR spectra and PXRD),[10] the slow redistribution of pyridine in the pores of **1** is more probable.

[a] *Department of Chemistry, Texas A&M University, College Station, TX 77843, United States.*
[b] *Department of Materials Science and Engineering, Texas A&M University, College Station, TX 77843, United States.*

Electronic Supplementary Information (ESI) available: Experimental details and supporting data (PDF). See DOI: 10.1039/x0xx00000x

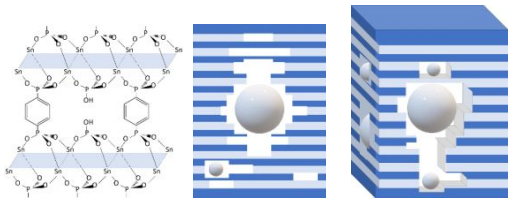

Figure 1. Idealize structure of compound **1** with the formula $Sn(O_3PC_6H_4PO_3)_{0.85}(O_3POH)_{0.30}$ (left). The pore formation in the macro structure of **1**: a 2D image where the blue and grey spaces are Sn and organic layers (middle) and a 3D image with an idealized smooth pore surface where grey units symbolize pore sizes (right).

This conclusion is supported by the $^{31}P\{^1H\}$ and $^{119}Sn\{^1H\}$ MAS NMR data (SI) for materials **1-Py-1.6**, **1-Py-0.6**, and **1-Py-0.2**, which are summarized in Table S1 and Figure S1. These data show that at varying the pyridine amounts and sample temperatures, the isotropic chemical shifts of target nuclei, corresponding to a SnO_6 octahedral environment do not change.[14] This observation is particularly significant for the ^{119}Sn nuclei, which have a well-known large diapason of chemical shift. In addition, the ^{31}P T_1 values for the phosphonate and phosphate groups at room-temperature for material **1-Py-1.6** were 17.6 s and 14.1 s, respectively, which are close to those obtained for **1** (19.3 s and 14.6 s, respectively). Since these phosphorus relaxation times are governed by fast rotations of phosphonate and phosphate groups around P-Ph and P-OH bonds[15,16] these structural elements do not change in the presence of the pyridine.

The molecular dynamics of the pyridine in pores of **1-Py-1.6** and **1-Py-0.6** are investigated here by their static ^2H NMR spectra, shown in Figures 2A, and Figure S2. All of these show that on cooling the sharp pyridine resonance, transforms to the full-size Pake pattern of a quadrupolar C–D tensor, which indicates immobile pyridine molecules.[10] In fact, the same static quadrupole pattern has been reported for the bulk immobile pyridine at 77 K.[17] It should also be added that the ^2H NMR spectra of **1-Py-0.6** and **1-Py-1.6** are very similar (Figure S3) and the chemical exchange between the central component (*liquid-like pyridine*) and the quadrupolar pattern (*immobile molecules*) is slow on the NMR time scale; in other words, these states do not mix and can be well characterized separately.

To understand better the nature of the sharp ^2H resonance observed for **1-Py-1.6** and **1-Py-0.6** at 295 K, we compared the static ^2H NMR spectra of **1** containing acetone-d_6, acetonitrile-d_3, water-d_2, benzene-d_6 and pyridine-d_5 (Figure S4). In this comparison, all of the resonances were sharp, but had different linewidths: 0.58 kHz, 0.32 kHz, 0.63 kHz, 1.06 kHz and 3.56 kHz, respectively. The ^2H T_2 time, measured for pyridine-d_5 was 0.094 ms, which predicts a linewidth of 3.4 kHz via $\Delta\nu = 1/\pi T_2$, in excellent agreement with the empirical result. Similarly, the water resonance in sample **1-D_2O** shows a longer ^2H T_2 time of 0.6 ms, again in good agreement with the direct measurement. Thus, the resonances observed are actually Lorentz-shaped, corresponding well to liquid-like molecules, moving isotropically within pores.

Since the linewidth of the pyridine signal remained the same for **1-Py-1.6** and **1-Py-0.6** spinning at a rate of 9 kHz, the observed linewidth can be attributed to a fast exchange between "free" (liquid-like) pyridine molecules and bound pyridine molecules moving anisotropically. This conclusion is supported well by strong consistent broadenings of isotropic resonances in the variable-temperature ^2H MAS NMR spectra of **1-Py-0.6** (Figure 2A) and **1-Py-1.6** (Figure S2).

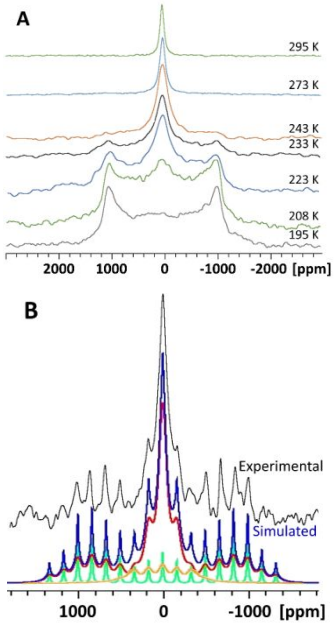

Figure 2. (A): a part of the static variable-temperature solid-echo ^2H NMR spectra recoded for **1-Py-0.6**; (B): the 205 K ^2H MAS NMR spectrum, recorded at a spinning rate of 10.5 kHz, simulated as patterns with C_Q of 180 kHz at asymmetry parameter η of 0.08 (green), C_Q of 180 kHz at η of 0.08 for deuterium in para-position (orange) and C_Q of 25 kHz at η of 0.12 for other C–D bonds (red) to give the total line (blue).

The first candidate for the bound mobile states (besides the above-mentioned immobile molecules) is pyridine molecules adsorbed on the pore surface, experiencing the well-known fast (out of the NMR time scale) in-plane C_6 rotation as shown in Figure 3 as state **A** (ref. 10 and references there).

This situation spectroscopically corresponds to a quadrupolar pattern with a quadrupole coupling constant (C_Q) of 90 kHz shown in Figure S5A. The second mobile state can involve molecules bonding to the pore surface, for example, by hydrogen bonds [18-19] that allow fast rotation (state **B** in Figure 3). This fast rotation does not affect the static C_Q of 180 kHz for the C–D bonds lying on this bond axis, but the other C–D bonds, which form the angle of 60° (θ) relative to the rotational axis, will show a reduced C_Q to 23 kHz via the equation: $\Delta\nu$ (splitting) = ¾ 180 (kHz)$(3\cos^2\theta\text{-}1)/2$.[20] This spectroscopic situation is also shown in Figure S5B. It is evident that direct independent observation of both mobile states of the pyridine in low-temperature *static* ^2H NMR spectra is impossible. The complication is due to the presence of the highly-intense static quadrupolar resonance of immobile pyridine molecules. To facilitate the observation, the 205 K MAS NMR spectrum of **1-Py-0.6** was recorded at spinning rates of 10.5 (Figure 2B).

The simulations of this spectrum (Figure 2B) revealed again a quadrupolar pattern of immobile pyridine molecules with a quadrupole coupling constant (C_Q) of 180 ± 3 kHz at η = 0.08 and in addition minor quadrupolar patterns of *mobile* pyridine with a C_Q of 180 kHz at η of 0.08 for deuterium in para-position

and C_Q of 25 ± 2 kHz (η = 0.12) for other C–D bonds. Since this value is very close to 23 kHz, mentioned above, only bound state **B** shown in Figure 3 was found experimentally.

Table S2 and Figure S6 show the temperature dependent linewidths in the ^{2}H NMR spectra of **1-Py-0.6**. They demonstrate the above-mentioned chemical exchange between the isotropically- and anisotropically-moving pyridine molecules.

This dependence, Δν (kHz) versus T(K), clearly falls to two distinct sections: a high temperature zone where the Δν grows moderately on cooling, and a low temperature zone characterized by a strong Δν increase. The high temperature zone corresponds to a very fast chemical exchange, occurring out of the NMR time scale, while the second section illustrates exchange on the NMR time scale, which affects line shapes of the resonances.

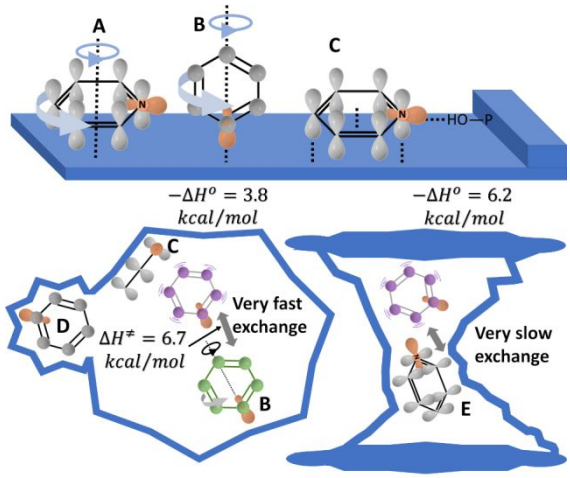

Figure 3. Schematic representation of the pore spaces in **1-Py-0.6**, top view (left) and side view (right), and pyridine molecular motions, where violet symbols are molecules moving isotropically; **top**: bound mobile pyridine molecules with fast in-plane C_6 rotation (**A**); mobile fast rotating pyridine molecules binding to the pore surface via hydrogen bonds O-H···N (**B**); immobile molecules on the pore surface (**C**), in cavities (**D**) and in spatially restrictive pore places (**E**).

The high temperature diapason can be treated to obtain mole fractions of bound pyridine molecules, P_b, via the equation (1),[21] where $\Delta\nu_{obs}$ is the observed linewidth, $\Delta\nu_{free}$ is the linewidth, characterizing liquid-like

$$\Delta\nu_{obs}=\Delta\nu f_{ree}+P_b\Delta\nu_b \quad (1)$$

pyridine molecules (taken as 0.4 kHz used earlier for free benzene in[10] and $\Delta\nu_b$ is the linewidth of bound pyridine molecules taken as 18 kHz (i.e. as $\Delta\nu_{(splitting)}$ = ¾C_Q at C_Q of 25 kHz), corresponding to fast rotating molecules **A** in Figure 3. The temperature-dependent equilibrium constants, $K_{eq}P_b/P_{free}$, in Table S2, presented in the coordinates ln(K_{eq}) versus 1/T give a enthalpy change (-ΔH°) of 3.8 kcal/mol that characterizes adsorption of the pyridine molecules in pores of material **1-Py-0.6** via hydrogen bonds (states **B**). As noted above, the variable-temperature ^{2}H NMR spectra in the low temperature zone (Table S2 and Figure S6) may be used to characterize the kinetics of the exchange between free and bound pyridine molecules in the pores by line shape analysis. This exchange, occurring on the NMR time scale was treated with a three-center model where the frequency distance of outer resonances is taken as 18 kHz, corresponding to two main singularities of the above mobile pyridine (with C_Q of 25 kHz) and a central resonance that belongs to the free pyridine molecules (Figure S7). The fitting procedures lead to the rate constants $k_{(exch)}$ in Table S2, and the corresponding temperature dependence in the coordinates ln($k_{(exch)}$) versus 1/T yield an activation enthalpy change ($\Delta H^{\neq}$) of 6.7 kcal/mol. An activation energy ΔE_a of 1.6 kcal/mol, has been determined by ^{2}H T_1 time measurements that characterizes the isotropic resonance of pyridine-d_5 in the pores of **1**.[10] Such low ΔE_a values are typical of isotropic motions in liquids, and have been reported in the microporous metal–organic compound Zn_4O-($O_2CC_6H_4CO_2$)$_3$, (MOF-5).[22] Furthermore, this activation energy, via equation $\Delta E_a = \Delta H^{\neq} + RT$, gives $\Delta H^{\neq}$ of 1.1 kcal/mol at 263 K, which is significantly smaller than that found for the above exchange. This difference is due to interactions between bound pyridine molecules and pore walls.

Finally, immobile pyridine molecules in pores of **1-Py-0.6** have been characterized thermodynamically by determination of mole fractions (P_{immob} and P_{mob}) via integration in the ^{2}H NMR spectra and the corresponding equilibrium constants, K_{eq} = P_{immob}/P_{mob}, shown in Table S3. A plot ln(K_{eq}) versus 1/T indicates an enthalpy change (-ΔH°) of 6.2 kcal/mol. The thermodynamic and kinetic data are presented in Figure 3, which illustrates our understanding the behaviour of the pyridine molecules in the pores of **1**.

One significant feature of this system is the appearance of the solid-like pyridine signal in the ^{2}H NMR spectra at temperatures higher than the melting point (Figure 2 and S2). This is in contrast to the well-known melting point depression typical of guest molecules in porous materials.[23] Nevertheless, very similar behaviour of pyridine has been recently reported for metal-organic frameworks MIL-100(Al), where pyridine molecules coordinate to the Al-OH sites.[18] However, it is interesting that the activation energy found for the exchange between the bound and isotropically-moving states of pyridine in MIL-100(Al) was 3.6 kcal/mol[18], which is remarkably smaller than 6.7 kcal/mol noted above. As detailed below, potential hydrogen bonding (O-H···N) is possible in the pores of **1**, which could explain why the -ΔH° characterizing the solid-like pyridine in **1-Py-0.6** is larger the enthalpy changes for fusion of bulk pyridine (2 kcal/mol). According to one hypothesis,[8] the pores in metal (IV) phosphate-phosphonates develop by the coming together of layers with different sizes (Figure 1), where the end groups, phosphonic acid moieties and/or P-OH phosphate groups, form pore spaces in **1**. In this mechanism, the pores formed with cavities and protrusions will be differently-sized and "imperfect" pore surfaces will be covered by acidic OH groups, which coordinate the fast-rotating bound pyridine molecules via hydrogen (O-H···N) bonds with the formation enthalpy of 3.8 kcal/mol (state **B** in Figure 3).

We believe that these molecules, capable of fast exchange with free pyridine are rather located on *protrusions* in pores. The latter provides their fast rotations. Note that since Sn atoms in **1** are six-coordinated, they are not involved into the Sn···N interactions. The observation of immobile (spectrally solid-like) pyridine at high temperature in the ^{2}H NMR spectra of **1-Py-1.6** and **1-Py-0.6** can be explained by the pyridine molecules which form hydrogen bonds with OH protons of the surface and are located in narrow cavities of the pores (state **D**, Figure 3). These

cavities obviously will restrict their motions. On cooling, N···H-bonding, H…π(electron) interactions with the pore surface and also dipole-dipole interactions between pyridine molecules (μ = 2.3D) form the immobile solid-like pyridine (state **C**, Figure 3). The spectral behaviour of material **1-Py-0.2**, obtained by 6 hours heating of **1-Py-0.6** at 150° C, provides additional information about the shapes of pores in **1**. Figure 4 shows room-temperature ^{2}H NMR spectra of freshly obtained material **1-Py-0.2**, where the major component is immobile solid-like pyridine (state **E** in Figure 3). In fact, the spectrum obtained at 10 kHz can be reproduced in Figure S8 using the full quadrupolar pattern with C_Q of 178±2 kHz (η = 0.12) in the presence of a minor pattern with C_Q of 40±2 kHz (η = 0.15). Such pyridine behaviour with restricted motions has also been observed at room temperature in mesoporous silica materials.[19]

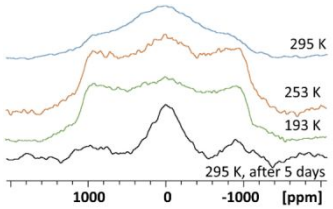

Figure 4. The static ^{2}H NMR spectra of material **1-Py-0.2** from top to bottom: the freshly-obtained material at 295 K, 253 K and 193 K; the room-temperature static spectrum collected after five days.

As seen in Figure 4, with cooling the spectrum does not change unexpectedly. However, the **1-Py-0.2** signal slowly changes (over days): the solid-like pyridine signal reduces and the central component (liquid-like pyridine) increases. Since the ^{31}P and ^{119}Sn NMR spectra of **1-Py-0.2** do not change over time, Figure 4 reflects the redistribution of pyridine guest molecules from spatially restrictive places to more open, larger pore spaces, which must be connected. In other words, the pores in **1** are not 'cylindrical' narrowing in some places or they can be connected via narrow channels. This situation can be better represented as shown in Figure 3.

In summary, we have shown that applications of multi-nuclear solid-state NMR techniques with pyridine-d_5 as a probe, provide reliable macrostructure and pore shape information of compound **1**, as a representative of phosphonate-phosphate materials. Five states of pyridine were found: immobile pyridine in cavities, immobile pyridine in spatially restrictive pore places, immobile solid-like pyridine on the pores surface, the bound fast-rotating pyridine and free pyridine molecules. It should be added that the behaviour of first three states is spectrally identical and only additional experiments provide their discrimination.

Conflicts of interest

There are no conflicts to declare.

Acknowledgments

This work was supported by the Robert A. Welch Foundation Grant A-0673, the Nuclear Energy University Program (DOE) (DE-NE0000746) and the U.S. Department of Energy (DOE), Basic Energy Sciences (DE-SC0017864), for which grateful acknowledgement is made. H.-C.Z. acknowledges support from the Robert A. Welch Foundation (A-0030).

References

1 C. V. Kumar, Bhambhani A., Hnatiuk Nathan E., in Handbook *Layered materials*, ed. S. M. Auerbach, K. A. Carrado, P. K. Dutta, Marcel Dekker, Inc., New York, Basel, **2004**.
2 A. Diaz, V. Saxena, J. Gonzalez, A. David, B. Casanas, C. Carpenter, J. D. Batteas, J. L. Colon, A. Clearfield and M. D. Hussain, *Chem Commun*, 2012, **48**, 1754-1756.
3 A. Diaz, M. L. Gonzalez, R. J. Perez, A. David, A. Mukherjee, A. Baez, A. Clearfield and J. L. Colon, *Nanoscale*, 2013, **5**, 11456-11463.
4 F. Costantino, R. Vivani, M. Bastianini, L. Ortolani, O. Piermatti, M. Nocchetti and L. Vaccaro, *Chem Commun*, 2015, **51**, 15990-15993.
5 R. Silbernagel, T. C. Shehee, C. H. Martin, D. T. Hobbs and A. Clearfield, *Chem. Mater.*, 2016, **28**, 2254-2259.
6 S. B. Cahill R., Peng G.-Z., Bortun L., Clearfield A., in Separations of *f* Elements, ed. G. R. C. K.L. Nash, Plenum Press, New York, 1995, pp. 165-176.
7 J. D. Burns, A. Clearfield, M. Borkowski, D. T. Reed, *Radiochim Acta* 2012, **100** (6), 381-387.
8 A. Clearfield, Z. K. Wang, *J Chem Soc Dalton* 2002, (15), 2937-2947.
9 R. Silbernagel, C. H. Martin, A. Clearfield, *Inorg Chem* 2016, **55** (4), 1651-1656.
10 V. I. Bakhmutov, D. W. Elliott, A. R. Contreras, A. Clearfield, *J Phys Chem A* 2018, **122** (51), 9901-9909.
11 M. J. Duer (Editor) Solid-state NMR spectroscopy, principles and applications, Blackwell Science, Oxford, **2002**.
12 A. R. Contreras, V. I. Bakhmutov, D. W. Elliott, A. Clearfield, *Magn Reson Chem* 2018, **56** (12), 1158-1167.
13 D. I. Kolokolov, H. Jobic, S. Rives, P. G. Yot, J. Ollivier, P. Trens, A. G. Stepanov, G. Maurin, *J Phys Chem C* 2015, **119** (15), 8217-8225.
14 M. D. Gomez-Alcantara, A. Cabeza, P. Olivera-Pastor, F. Fernandez-Moreno, I. Sobrados, J. Sanz, R. E. Morris, A. Clearfield, M. A. G. Aranda, *Dalton Trans* 2007, (23), 2394-2404.
15 V. I. Bakhmutov, A. Clearfield, *J Phys Chem C* 2017, **121** (1), 550-555.
16 J. A. Sheikh, V. I. Bakhmutov, A. Clearfield, *Magn Reson Chem* 2018, **56** (4), 276-284.
17 R. G. Barnes, J. W. Bloom, *J Chem Phys* 1972, **57** (8), 3082-3086.
18 A. E. Khudozhitkov, A. V. Toktarev, S. S. Arzumanov, A. A. Gabrienko, D. I. Kolokolov, A. G. Stepanov, *Chem Eur J* 2019, **25** (46), 10808-10812.
19 G. Buntkowsky, H. Breitzke, A. Adamczyk, F. Roelofs, T. Emmler, E. Gedat, B. Grunberg, Y. P. Xu, H. H. Limbach, I. Shenderovich, A. Vyalikh, G. Findenegg, *Phys Chem Chem Phys* 2007, **9** (35), 4843-4853.
20 M. Gielen, R. Willem, B. Wrackmeyer, *Unusual Structures and Physical Properties in Organometallic Chemistry*. West Sussex, Wiley **2002**.
21 M. L. Martin, J. J. Delpuech, G. J. Martin, *Practical NMR spectroscopy*. Heyden & Sons: London, **1980**.
22 J. Gonzalez, R. N. Devi, D. P. Tunstall, P. A. Cox, P. A. Wright, *Micropor Mesopor Mat* 2005, **84** (1-3), 97-104.
23 L. D. Gelb, K. E. Gubbins, R. Radhakrishnan, *Rep Prog Phys* 1999, **62** (12), 1573-1659.